*Kovove Mater. 56 2018 171–175*
*DOI: 10.4149/km_2018_3_171*



# Characterization of $CuInSe_2$ films prepared by spin-coating and chemical co-reduction with nitrates

J. Li[1,2], P. B. Cui[2,1], K. G. Liu[2,1]*, Y. Xu[2], L. Zhang[2]

[1] *Co-Innovation Center for Green Building of Shandong Province, Shandong Jianzhu University, Fengming Road, Jinan 250101, P. R. China*
[2] *School of Materials Science and Engineering, Shandong Jianzhu University, Fengming Road, Jinan 250101, P. R. China*

Received 23 April 2018, received in revised form 13 May 2018, accepted 22 May 2018

**Abstract**

$CuInSe_2$ films were prepared by spin-coating and chemical co-reduction method using $Cu(NO_3)_2 \cdot 3H_2O$, $In(NO_3)_3 \cdot 4.5H_2O$, and $SeO_2$ powders as raw materials, and the reaction mechanism was analyzed. The phases of product samples were analyzed by X-ray diffraction (XRD) on the Bruker D8 Advance XRD system with Ni-filtered Cu-K$\alpha$ ($\lambda$ = 1.5059 Å). The surface resistance of the product film was measured using a four-probe resistance instrument. The surface morphology of the product films was observed using scanning electron microscope (SEM). The experimental results show that the film samples can be prepared at 140–220 °C with major phase $CuInSe_2$ which diffraction peaks at 2$\theta$ angles with 26.7°, 44.3°, and 52.5° correspond to the (112), (204), and (312) crystal planes, respectively. With the increase of the reaction temperature, the diffraction peak intensity of $CuInSe_2$ increases and the crystallization becomes better. The $CuInSe_2$ film samples obtained at 200 and 220 °C for 20 h consist of round crystals with diameters of about 0.3–0.5 μm and a small number of large crystals with diameters of about 1–1.5 μm. The reaction time prolongation facilitates the crystallization of the thin film samples. The average resistivity of $CuInSe_2$ film synthesized at 220 °C for 40 h was 4.18 $E^{-3}$ Ω cm.

K e y w o r d s: photoelectric film, co-reduction, spin-coating, resistivity, $CuInSe_2$

## 1. Introduction

$CuInSe_2$ is one of the promising second-generation photovoltaic materials since it has a direct bandgap structure and suitable forbidden bandwidth. It has many advantages such as excellent absorption coefficient, good spectral response characteristics, low manufacturing cost, and reliable stability. So $CuInSe_2$ has become a research hotspot of photovoltaic materials [1, 2]. $CuInSe_2$ has a large absorption coefficient and a bandgap width of 1.04 eV that is well matched to the solar spectrum. Because there is no photo-induced decay, CIS thin-film photovoltaic cells also have reliable stability. In addition, $CuInSe_2$ has good chemical compositional fault tolerance in the preparation process, which can tolerate the deviation of less than 5 % in molar fraction [3], that is, when the atomic ratio of Cu, In, and Se deviates from the normal ratio 1 : 1 : 2, the chalcopyrite structure can still be formed and still has similar physical and chemical properties. The synthesis methods of CIS films are roughly divided into vacuum technology and non-vacuum technology. Vacuum technologies mainly include sputtering [4, 5] and co-evaporation [6, 7], non-vacuum technologies mainly include electrodeposition [8], spray pyrolysis [9], and co-reduction [10], etc. In this work, $CuInSe_2$ films were prepared by spin-coating and chemical co-reduction method. The equipment is simple and easy to operate. The effects of the different reaction temperature and reaction time on phase formation, crystallization, grain size, and surface morphology of $CuInSe_2$ films were investigated, and the reaction mechanism of $CuInSe_2$ synthesis was analyzed.

*Corresponding author: tel.: +86-15610183153; e-mail address: liukg163@163.com


Fig. 1. The process chart for preparing a $CuInSe_2$ film by spin-coating and chemical co-reduction.

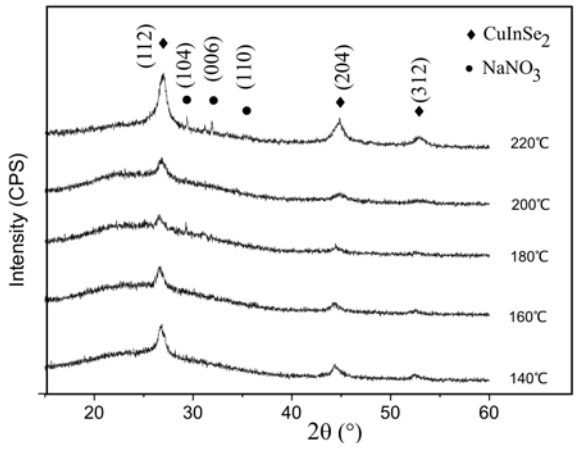


Fig. 2. XRD patterns of $CuInSe_2$ samples prepared at different reaction temperatures for 20 h.

## 2. Experimental

The main experimental operations are: the glass substrate was cut into squares with side length 3 cm using a sapphire plate and boiled in sulfuric acid solution for 20 min. Then it was put into anhydrous ethanol and shaken for 20 min and dried. $Cu(NO_3)_2 \cdot 3H_2O$, $In(NO_3)_3 \cdot 4.5H_2O$, and $SeO_2$ powders were placed in the glass bottle and dissolved in ethanol under ultrasonic vibration to make into light green or blue precursor solutions. The precursor films with certain thickness were obtained by spin-coating with the precursor solution and drying. The precursor films were placed in a Teflon-lined steel reactor vessel, and 1 mL of hydrazine hydrate was added as a reducing agent. The grayish-black film samples were obtained by heating the sealed steel reactor at 140–200 ℃ for 20–40 h. The experimental processes are shown in Fig. 1.

The elemental compositions of the product films were analyzed by the online energy spectrum analyzer with scanning electron microscope (EDS). The phases of product samples were analyzed by X-ray diffraction (XRD) on the Bruker D8 advance XRD system with Ni-filtered Cu-K$\alpha$ ($\lambda$ = 1.5059 Å). The surface resistance of the product film was measured using a four-probe resistance instrument. The surface morphology of the product films was observed using scanning electron microscope (SEM) with a model of JSM-6380LA made by Japan Electronics Co., Ltd.

## 3. Experimental results and discussion

### 3.1. The phase and morphology of $CuInSe_2$ films prepared at different temperatures

Figure 2 shows the XRD patterns of $CuInSe_2$ samples prepared by spin-coating and chemical co-reduction method with nitrates and $SeO_2$ as raw materials at different reaction temperatures for 20 h. It can be seen that the XRD peaks of the samples can correspond to the $CuInSe_2$ standard PDF card with No.65-4105, where the XRD peaks at 2$\theta$ angles with 26.7°, 44.3°, and 52.5° correspond to (112), (204), and (312) crystal planes, respectively. Also, some XRD peaks correspond to the $NaNO_3$ standard PDF card with No.72-25. The XRD peaks for $NaNO_3$ at 2$\theta$ angles with 29.4°, 31.9°, and 35.4° correspond to the (104), (006), and (110) planes, respectively. Compared with the XRD curves obtained at different temperatures, it can be found that as the reaction temperature increases, the intensity of the XRD peak continuously increases. In addition to the target product $CuInSe_2$, a small amount of $NaNO_3$ impurities appear.

Figure 3 shows the SEM images of $CuInSe_2$ films prepared with nitrates and $SeO_2$ for 20 h at different reaction temperatures. Figures 3a,b are the images of the sample obtained at 200 ℃. It can be seen that it consists of round crystals with diameters of about 0.3–0.5 μm and a small number of large crystals with a diameter of about 1–1.5 μm. Figures 3c,d show the images of the sample obtained at 220 ℃. This film sample is relatively dense and consists of round crystals with diameters of about 0.3–0.5 μm and a small number of large crystals with diameters of about 1–2.5 μm.

### 3.2. The phase and morphology of $CuInSe_2$ films

Figure 4 shows the XRD patterns of $CuInSe_2$ film samples prepared by spin-coating and chemical co-reduction with nitrates and different reaction time. The curves a and b in Fig. 4 are the XRD patterns of the samples obtained at 220 ℃ for 40 h and 20 h, respectively. The diffraction peaks in Fig. 4 correspond to the $CuInSe_2$ standard PDF card with No.65-4105, in which the diffraction peaks at 2$\theta$ angles with 26.7°, 44.3°, and 52.5° correspond to (112), (204), and (312) crystal planes, respectively. Also, the curve b can correspond to the $NaNO_3$ standard PDF card with No.72-25, where the diffraction peaks at 2$\theta$ angles with 29.4° and 31.9° correspond to (104) and

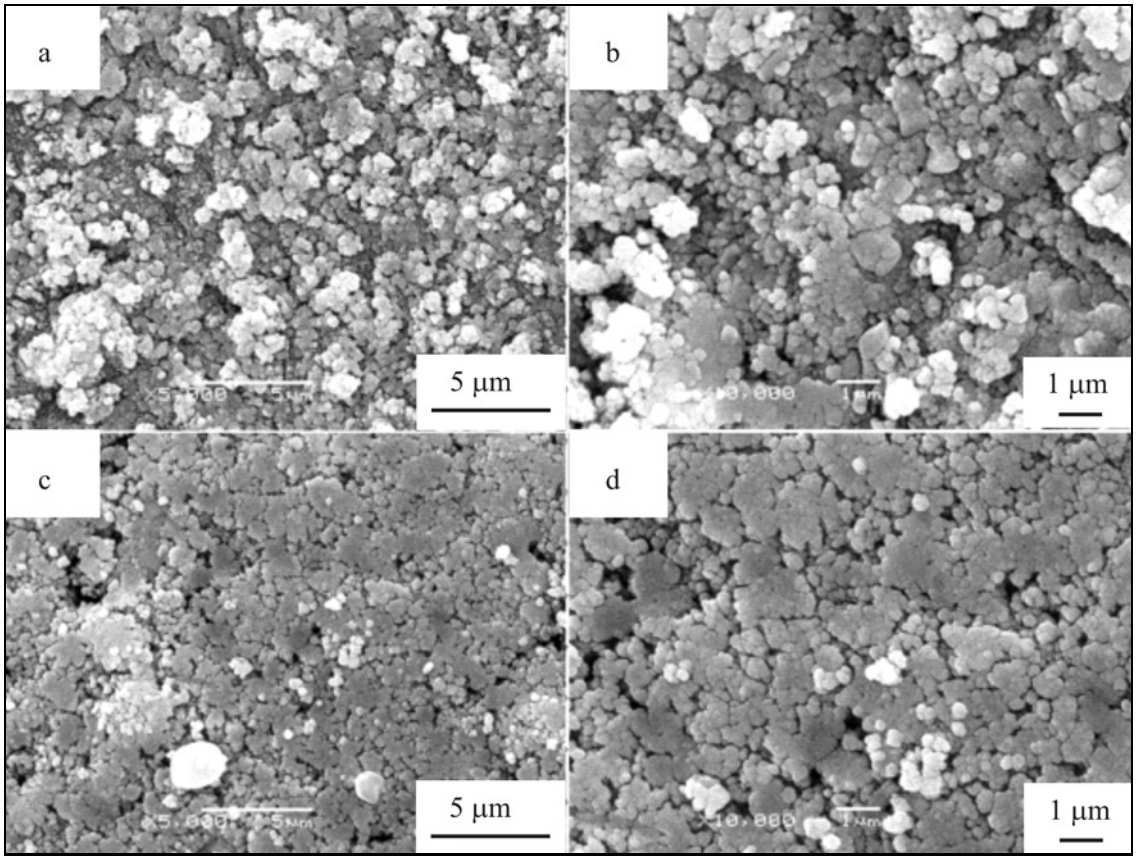


Fig. 3. SEM images of $CuInSe_2$ samples prepared with nitrates and $SeO_2$ at different temperatures.

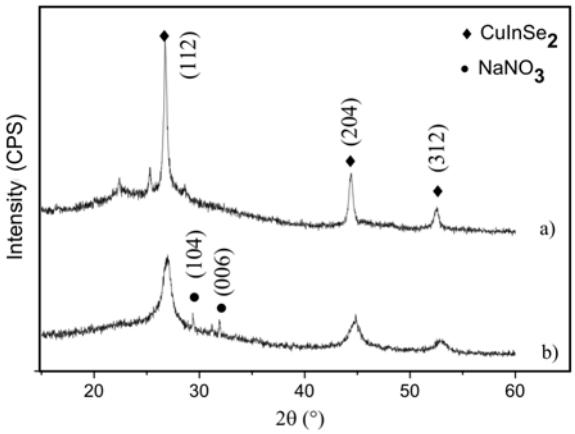


Fig. 4. XRD patterns of $CuInSe_2$ samples prepared with different reaction time.

(006) crystal planes, respectively. Comparing with the two XRD curves, it can be found that the sample obtained with 40 h has sharper shape and higher peaks in intensity, and no diffraction peaks which correspond to the $NaNO_3$ standard PDF card with No.72-25, which indicates that it contains no impurity $NaNO_3$.

Figure 5 gives the SEM images of the product samples prepared by spin-coating and chemical co-reduction using nitrates as raw materials at 220 ℃. Figures 5a,b are the SEM images of the sample obtained with reaction time 20 h. This dense sample consists of round crystals with diameters of about 0.3–0.5 μm and a small number of large crystals with diameters of about 1–2.5 μm. Figures 5c,d show the SEM images of the sample obtained with reaction time 40 h. It can be seen that the product film is still composed of round crystals with diameters of about 0.3–0.5 μm, but no more large crystals appear.

### *3.3. Composition analysis of the $CuInSe_2$ film*

Figure 6 shows the EDS image of the sample obtained with nitrates as raw materials at 220 ℃ for 40 h. It can be seen that it contains Cu, In, and Se elements. The other elements are contained in the glass substrate.

### *3.4. Analysis of electrical properties of $CuInSe_2$ films*

Table 1 shows the electrical properties of the $CuInSe_2$ film prepared with nitrates as raw materials at 220 ℃ for 40 h. The average resistivity is $4.18\,E^{-3}\,\Omega\,cm$.

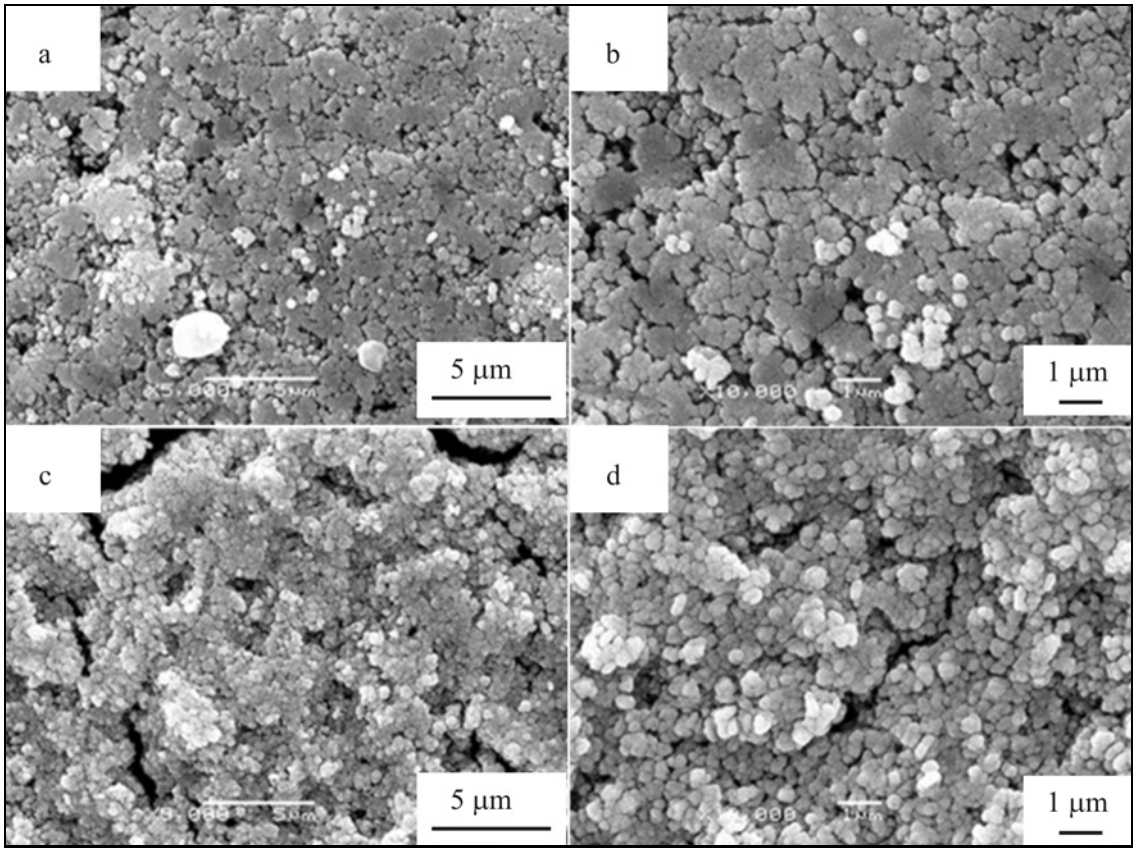


Fig. 5. SEM images of $CuInSe_2$ samples prepared with different reaction time.

Table 1. The electrical properties of the $CuInSe_2$ film prepared with nitrates at 220 ℃ for 40 h

| Points | Forward voltage (mV) | Reverse voltage (mV) | Resistivity (Ω cm) | Conductivity ($S\,cm^{-1}$) |
|---|---|---|---|---|
| 1 | 21.02 | 20.78 | 4.18 $E^{-3}$ | 239.23 |
| 2 | 21 | 20.77 | 4.18 $E^{-3}$ | 239.23 |
| 3 | 21 | 20.76 | 4.18 $E^{-3}$ | 239.23 |
| 4 | 21.03 | 20.79 | 4.18 $E^{-3}$ | 239.23 |
| 5 | 21.02 | 20.78 | 4.18 $E^{-3}$ | 239.23 |
| 6 | 21.02 | 20.77 | 4.18 $E^{-3}$ | 239.23 |

### *3.5. Analysis of synthesis mechanism of $CuInSe_2$ films*

Using nitrates and selenium dioxide as raw materials, anhydrous ethanol as the solvent, hydrazine hydrate as the reducing agent, $CuInSe_2$ films were synthesized by spin-coating and chemical co-reduction method. The chemical reaction equations are as follows:

$$Cu(NO_3)_2 \cdot 3H_2O + N_2H_4 \cdot H_2O \rightarrow Cu + 2HNO_3 + N_2\uparrow + 3H_2O + H_2\uparrow, \quad (1)$$

$$SeO_2 + H_2O \rightarrow H_2SeO_3, \quad (2)$$

$$H_2SeO_3 + N_2H_4 \cdot H_2O \rightarrow Se + N_2\uparrow + 4H_2O, \quad (3)$$

$$2In(NO_3)_3 \cdot 4.5H_2O + 2N_2H_4 \cdot H_2O \rightarrow 2In + 6HNO_3 + 2N_2\uparrow + 11H_2O + H_2\uparrow, \quad (4)$$

$$Cu + 2Se + In \rightarrow CuInSe_2. \quad (5)$$

## 4. Summary

$CuInSe_2$ films were prepared by spin-coating and chemical co-reduction method using $Cu(NO_3)_2 \cdot 3H_2O$, $In(NO_3)_3 \cdot 4.5H_2O$, and $SeO_2$ powders as raw materials. The film samples can be prepared at 140–220 ℃

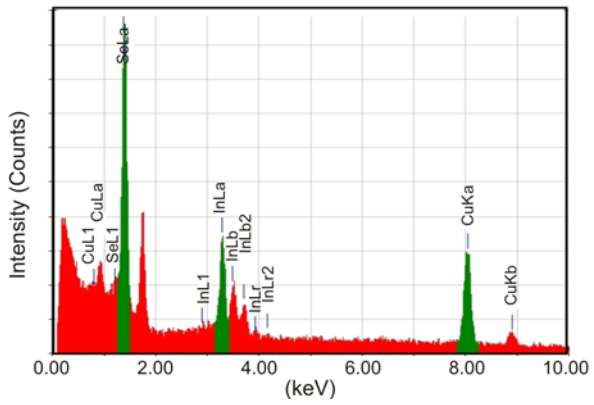


Fig. 6. The EDS image of the $CuInSe_2$ sample prepared with nitrates as raw materials at 220 ℃ for 40 h.

with major phase $CuInSe_2$ which diffraction peaks at $2\theta$ angles with 26.7°, 44.3°, and 52.5° correspond to the (112), (204), and (312) crystal planes, respectively. With the increase of the reaction temperature, the diffraction peak intensity of $CuInSe_2$ increases and the crystallization becomes better. The $CuInSe_2$ film samples obtained at 200 and 220 ℃ for 20 h consist of round crystals with diameters of about 0.3–0.5 μm and a small number of large crystals with diameters of about 1–1.5 μm. The reaction time prolongation facilitates the crystallization of thin film samples. The average resistivity of $CuInSe_2$ film synthesized at 220 ℃ for 40 h was 4.18 $E^{-3}$ Ω cm.

## Acknowledgement

This work was financially supported by the National Natural Science Foundation of China (No.51272140).

## References

[1] Sadewasser, S., Salomé, P. M. P., Rodriguez-Alvarez, H.: Sol. Energ. Mat. Sol. C., *159*, 2017, p. 496. doi:10.1016/j.solmat.2016.09.041
[2] Stephan, Ch., Greiner, D., Schorr, S., Kaufmann, Ch. A.: J. Phys. Chem. Solids, *98*, 2016, p. 309. doi:10.1016/j.jpcs.2016.07.022
[3] Li, Y. H., Ma, A. B., Zhang, K. X.: Materials Guide (China Journal), *28*, 2014, p. 136.
[4] Salomé, P. M. P., Cunha, A. F. D.: Advanced Materials Forum IV, *587–588*, 2008, p. 323. doi:10.4028/www.scientific.net/MSF.587-588.323
[5] Delahoy, A. E., Chen, L., Akhtar, M.: Sol. Energy, *77*, 2004, p. 785. doi:10.1016/j. solener.2004.08.012
[6] Moharram, A. H., Hafiz, M. M., Salem, A.: Appl. Surf. Sci., *172*, 2001, p. 61. doi:10.1016/S0169-4332(00)00836-9
[7] Klinkert, T., Jubault, M., Donsanti, F.: Thin Solid Films, *558*, 2014, p. 47. doi:10.1016/j.tsf.2014.02.071
[8] Hamrouni, S., Al Khalifah, M. S., Boujmil, M. F.: Appl. Surf. Sci., *292*, 2014, p. 231. doi:10.1016/j.apsusc.2013.11.123
[9] Deshmukh, L. P. S. R.: Sol. Energy, *86*, 2012, p. 1910. doi:10.1016/j.solener.2012.02.033
[10] Liu, Y., Kong, D., Li, J.: Energy Procedia, *16*, Part A, 2012, p. 217. doi:10.1016/j.egypro.2012.01.036